



HAL
open science

Sorption behavior of Zn(II) ions on synthetic apatitic calcium phosphates

Haroun Sebei, Doan Pham Minh, Ange Nzihou, Patrick Sharrock

► **To cite this version:**

Haroun Sebei, Doan Pham Minh, Ange Nzihou, Patrick Sharrock. Sorption behavior of Zn(II) ions on synthetic apatitic calcium phosphates. *Applied Surface Science*, 2015, 357 (Part B), p. 1958-1966. 10.1016/j.apsusc.2015.09.158 . hal-01609210

HAL Id: hal-01609210

<https://hal.science/hal-01609210>

Submitted on 20 Oct 2018

HAL is a multi-disciplinary open access archive for the deposit and dissemination of scientific research documents, whether they are published or not. The documents may come from teaching and research institutions in France or abroad, or from public or private research centers.

L'archive ouverte pluridisciplinaire **HAL**, est destinée au dépôt et à la diffusion de documents scientifiques de niveau recherche, publiés ou non, émanant des établissements d'enseignement et de recherche français ou étrangers, des laboratoires publics ou privés.

Sorption behavior of Zn(II) ions on synthetic apatitic calcium phosphates

Haroun Sebei^{a,*}, Doan Pham Minh^{a,*}, Ange Nzihou^a, Patrick Sharrock^{a,b}

^a Université de Toulouse, Mines Albi, CNRS, Centre RAPSODEE, Campus Jarlard, F-81013 Albi Cedex 09, France

^b Université de Toulouse, SIMAD, IUT de Castres, avenue Pompidou, 81104 Castres, France

A B S T R A C T

The synthesis, characterization and the reactivity of apatitic calcium phosphates (Ca-HA, chemical formula $\text{Ca}_{10}(\text{PO}_4)_6(\text{OH})_2$) is reported. Calcium carbonate (CaCO_3) and potassium dihydrogen orthophosphate (KH_2PO_4) were selected as economical starting materials for the synthesis of Ca-HA under atmospheric conditions. Monocalcium phosphate monohydrate (MCPM), dicalcium phosphate dihydrate (DCPD), and octacalcium phosphate pentahydrate (OCP) were identified as the main intermediates of the synthesis reaction. The product obtained after 48 h of reaction contains mainly low-crystalline Ca-HA and small amounts of other calcium phosphates such as octacalcium phosphate (OCP), B-type carbonate apatite (CAP), as well as unreacted calcium carbonate. This Ca-HA was found to be active for the removal of Zn^{2+} from an aqueous solution. Its sorption capacity reached up to 120 mg of Zn^{2+} per g of Ca-HA powder after 24 h of reaction. The monitoring of soluble Zn, Ca and P during the sorption experiment allowed characterizing the mechanism of Zn uptake. Dissolution–precipitation, ionic exchange and surface complexation are the three main mechanisms involved in the sorption processes. The contribution of these mechanisms is discussed in detail.

Keywords:

Apatitic calcium phosphates

Characterization

Sorption kinetics

Mechanism

Zinc

1. Introduction

The low solubility of apatite minerals that are stable over geologic time associated to the ability of these materials to bind various metal ions promotes their use for environmental purpose. Thus, calcium hydroxyapatite (Ca-HA, $\text{Ca}_{10}(\text{PO}_4)_6(\text{OH})_2$) is used for the removal of heavy metals from contaminated soils, wastewater or fly ashes [1–4]. Many studies of the sorption of metals by Ca-HA have been undertaken using Ca-HA particles in aqueous solutions contaminated with divalent metals like Zn^{2+} [5,6], Cd^{2+} [6,7] and Pb^{2+} [6,8]. These studies observed the ion exchange between Ca on Ca-HA surface and metal ion during metal fixation, but suggested mechanisms including surface complexation, dissolution–precipitation and co-precipitation can also be considered. The difficulty remains the relative contribution of each process in removing metals. The implication of these mechanisms in the case of Zn sorption is discussed in this research.

From a technico-economical point of view, the minimization of costs (sorbent production, operational conditions, etc.) plays a

crucial role for the viability of a given environmental process. The use of inexpensive reagents, and associated with soft reaction conditions for producing sorbents is a solution. The reuse of industrial wastes as economical starting materials seems to match well with this goal [9–12].

In the present work, the synthesis of Ca-HA solids has been carried out by neutralization method at room temperature under atmospheric pressure, using calcium carbonate (calcite, CaCO_3) powder and an aqueous solution of potassium dihydrogen orthophosphate (KH_2PO_4). CaCO_3 is naturally available as the cheapest calcium source. The Ca-HA based solid powder obtained from this synthesis was thoroughly characterized by various methods, in particular for determining the Ca/P ratio at different surface levels. Ca-HA powder was then used for the removal of Zn^{2+} from an aqueous solution. Zn was chosen as model trace metal because it is one of the most concentrated and recurrent metals which can be present in wastewater [13]. Zn plays an essential role in biological function but can be toxic at high concentrations [14]. The use of pure starting materials for the synthesis of sorbent facilitates the analysis and characterization of the final powder product, which allows correlating the relationship between its composition and its sorption performance. The kinetics of Zn sorption was studied and the mechanisms for Zn fixation were unraveled.

* Corresponding authors.

E-mail addresses: haroun.sebei@mines-albi.fr (H. Sebei), doan.phamminh@mines-albi.fr (D. Pham Minh).

2. Materials and methods

2.1. Ca-HA synthesis

Calcium carbonate powder (CaCO_3 , 98%, Fisher Scientific) and potassium dihydrogen orthophosphate (KH_2PO_4 , 99%, Fisher Scientific) were used for the synthesis of Ca-HA powder.

The reaction was carried out in a 1 L glass reactor thermostated at 25 °C. An aqueous solution of KH_2PO_4 at a concentration of 1.20 mol L⁻¹ was prepared. The calcite powder was progressively added into the solution of KH_2PO_4 . The final theoretical molar ratio of Ca to P was 1.67, which is characteristic for the stoichiometric phosphocalcic hydroxyapatite. This mixture was stirred for 48 h at a speed of 350 rpm with a helical propeller. During the reaction, the pH of the suspension was continuously measured with a Mettler Toledo MPC pH-meter and recorded using LabView software. Samples withdrawn from the reaction mixture and final powder were filtered on a 0.45 μm hydrophilic filter to separate liquid and solid phases. The solid was washed several times with permuted water, dried overnight at 105 °C and then ground before further analyses. The liquid phase was acidified with nitric acid to avoid all secondary precipitation from calcium cations and orthophosphate species present in the liquid phase [15].

2.2. Characterization methods

The analysis by X-ray diffraction (XRD) was conducted using a Philips X'Pert diffractometer with copper anti-cathode ($\lambda = 1.540560 \text{ \AA}$). The identification of crystalline phases was determined by comparing the patterns with JCPDS standards. Thermal analysis was performed using SDT Q600 equipment (TA instruments). About 20 mg of solid were heated under air flux at 20 °C/min in an alumina crucible in the temperature range of 30–1000 °C. Fourier transformed infra-red spectroscopy (FTIR) was performed using a SHIMADZU – 8400S spectrophotometer scanning between 4000 and 500 cm⁻¹ in the reflexion mode. Scanning electron microscopy (SEM) was performed with a Philips XL30 ESEM FEG equipped with an EDAX analyzer. X-ray photoelectron spectroscopy (XPS) analysis was conducted with a VG ESCALB MK-II electron spectrometer using an Mg K α X-ray source (1253.6 eV). The energy scale was internally calibrated by referencing the binding energy of the C1s peak at 284.6 eV for contaminated carbon. The elemental analysis of phosphorus, calcium and potassium in the liquid phase was carried out with inductively coupled plasma atomic emission spectroscopy (ICP-AES) on a HORIBA JobinYvonUltima 2.

The true density of the powder was measured by helium pycnometry (MICROMERITICS Accupyc 1330). The particles size distribution of Ca-HA powder was determined with a MALVERN Laser Mastersizer Hydro 2000 in liquid medium. The specific surface area of the particles was determined by nitrogen adsorption using the BET method (MICROMERITICS Gemini Vacprep 061). The adsorption–desorption isotherm was determined with a MICROMERITICS ASAP 2010 using nitrogen as gas adsorbate with the data collection from relative pressure (P/P^0) of 0.03–0.99.

2.3. Sorption study

Aqueous solution of zinc nitrate was prepared by dissolving zinc nitrate (p.a. grade from Fisher Scientific) in permuted water to obtain a 1500 ppm Zn(II) solution. The experiments of sorption kinetics were carried out in a stirred glass reactor containing 1000 mL of the prepared zinc nitrate solution. The experiment started by addition of 8 g of Ca-HA powder sorbent into the reactor under constant stirring (350 rpm) at room temperature (ca. 25 °C). The contact time chosen for all sorption experiments was 24 h, which was considered to be sufficient to get apparent

equilibrium, as well as according to the literature [8,16]. Each sorption experiment was followed by filtration of the suspension through hydrophilic filter (0.45 μm), then the solid was washed, dried at 105 °C and then ground for further characterizations. The concentration of released Ca, P, K and remaining Zn ions in the equilibrium solution was quantified using the ICP-AES technique. During the sorption, the pH of the solution was continuously measured.

In order to calculate the amounts of metal ions sorbed by Ca-HA per mass unit, the following expression was used:

$$Q = (C^o - C^e) \times \left(\frac{V}{M} \right),$$

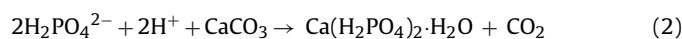
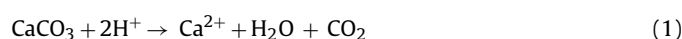
where Q is the amount of Zn^{2+} removed from the solution (mg of Zn per g of sorbent), C^o and C^e are the concentrations (mg L⁻¹) of Zn^{2+} in the initial zinc nitrate solution and at the sorption equilibrium, respectively, V (L) is the volume of the solution and M (g) the amount of Ca-HA used.

3. Results and discussion

3.1. pH evolution during synthesis

The initial orthophosphate solution had acid pH value of 4.2. When calcium carbonate was added, it reacted immediately with the acid solution, liberating carbon dioxide gas. Fig. 1 shows the evolution of recorded pH value during the first hour of reaction where three zones could be distinguished:

- Zone A:



The fast pH increase during the first minutes was due to the acid attack on the calcium carbonate powder (Eq. (1)) where free hydrated calcium cations (Ca^{2+}) were formed and protons were consumed. Then the first calcium phosphate compounds were formed by reaction between orthophosphate species and the calcium ions. At this early stage, monocalcium phosphate monohydrate (MCPM, $\text{Ca}(\text{H}_2\text{PO}_4)_2 \cdot \text{H}_2\text{O}$) was formed as the main calcium phosphate (Eq. (2)), because $\text{H}_2\text{PO}_4^{2-}$ is the main species at the pH of the solution in the zone A [10].

- Zone B:

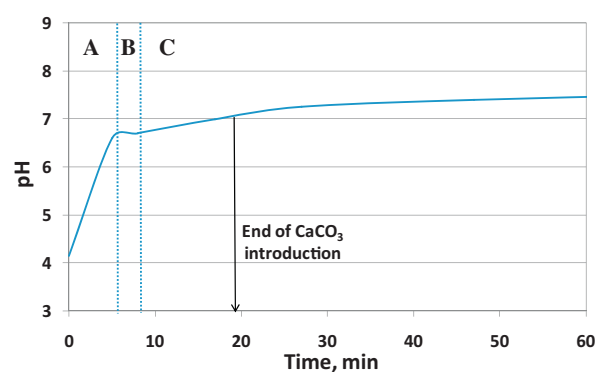
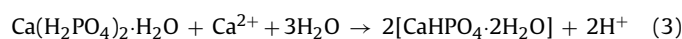


Fig. 1. pH evolution during the first 60 min of the reaction where calcium carbonate powder was progressively added into the potassium dihydrogen orthophosphate solution.

The next evolution has been identified as the transformation of MCPM into dicalcium phosphate dihydrate (DCPD, $\text{CaHPO}_4 \cdot 2\text{H}_2\text{O}$), as described by Eq. (3) [10]. This leads to the pH stabilization during few minutes (Zone B, Fig. 1). This is explained by the equilibrium between the consumption of protons (Eqs. (1) and (2)) and protons release (Eq. (3)).

- Zone C:

The pH increased slightly indicating the slow evolution of MCPM ($\text{Ca}(\text{H}_2\text{PO}_4)_2 \cdot \text{H}_2\text{O}$) and DCPD ($\text{CaHPO}_4 \cdot 2\text{H}_2\text{O}$) into other calcium orthophosphates [10]. At 48 h of reaction, the pH reached a value of 8.

3.2. ICP-AES analysis

The liquid fraction (filtrate) from the filtration of samples withdrawn from the medium during the synthesis was also analyzed by ICP-AES for the determination of soluble calcium and phosphate contents. Table 1 summarizes the results obtained.

For all the samples, low concentration of soluble calcium was observed. So, most of calcium can be found in solid form, either as calcium phosphates (CaP) or as undissolved calcium carbonate. For phosphate species, the conversion of phosphorus (X_p) was stagnated at about 72%, after 24–48 h of reaction. This limit may be due to the driving force induced by the presence of potassium ions (K^+) in solution, to counteract the ionic charge in aqueous phase [10].

Table 2 gives the results of elemental analysis of the solid product obtained after 48 h of reaction. The bulk molar ratio of Ca to P of the solid after 48 h of reaction was 2.38. But TG analysis (in the next section) shows that this solid product contains about 30 wt.% of CaCO_3 (Table 3). This means that among 355 mg g^{-1} of calcium determined by ICP-AES, there were 120 mg g^{-1} of calcium under remaining in calcite form. So there were maximum 235 mg g^{-1} of calcium under calcium phosphates forms. Thus, the calculated molar ratio of Ca to P of this solid was 1.58 for calcium phosphates. This suggests the formation of calcium-deficient apatites, such as octacalcium phosphate (OCP, $\text{Ca}_8\text{H}_2(\text{PO}_4)_6 \cdot 5\text{H}_2\text{O}$), as confirmed by

Table 1
Analysis of soluble phosphorus and calcium in the filtrate; X_p : conversion of initial phosphorus into solid calcium phosphate products.

Reaction time, h	[P], mmol/L	X_p , %	[Ca], mmol/L
0	1484	0	0
2	757	49	1.7
24	428	71	1.7
48	421	72	0.3

Table 2
Elemental composition of the solid powder obtained after 48 h of reaction.

Element	K, mmol g^{-1}	Ca, mg g^{-1}	Ca, mmol g^{-1}	P, mmol g^{-1}	Molar ratio of Ca to P
Content by ICP-AES	0.46 ± 0.01	355 ± 2	8.87 ± 0.04	3.72 ± 0.02	2.38 ± 0.01

Table 3
Evolution of calcium carbonate content remaining in the solid product calculated from the results of TG analysis.

Reaction time, h	CO_2 , wt%	Content of remaining CaCO_3 , %	CaCO_3 conversion (X_{CaCO_3}), %
0	43	100	0
2	21	49	51
24	13	30	70
48	13	30	70

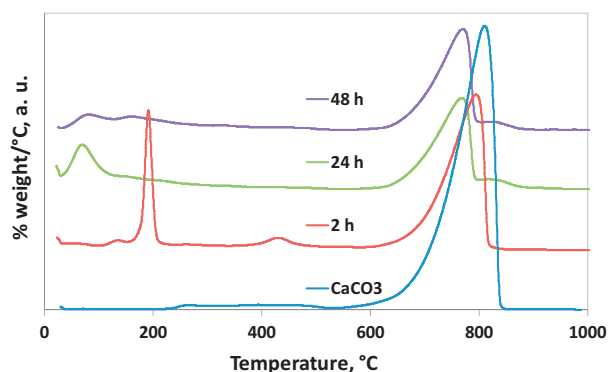


Fig. 2. Derivatives thermogravimetric (DTG) curves of pure CaCO_3 and Ca-HA powders after 2 h, 24 h and 48 h of reaction.

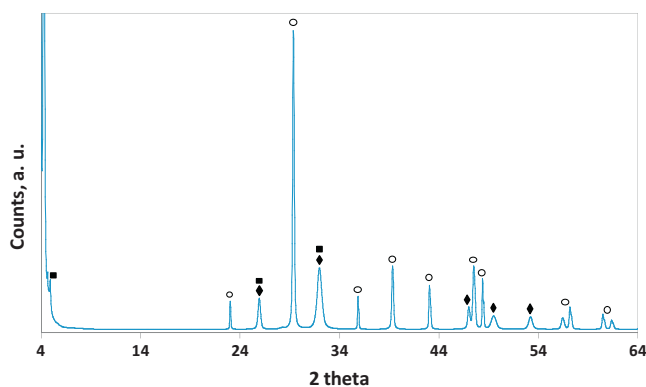


Fig. 3. XRD patterns of Ca-HA powder after 48 h of reaction, dried at 105°C . Principal diffractions of CaCO_3 (○); Ca-HA (◆); OCP (■).

XRD analysis (Section 3.4). Despite the washing of the solid several times with water, small amounts of potassium still remain in the final solid product. The potassium might exist in carbonate form (KHCO_3), or might be inserted into the apatitic structure [17].

3.3. TG analysis

Fig. 2 shows TG results obtained for the initial calcium carbonate and Ca-HA solids recovered at different reaction times. The weight loss at the temperature below 100°C is attributed to the elimination of physically absorbed surface moisture. Between 110 and 150°C , only the sample after 2 h of reaction shows a significant weight loss. This one is attributed to the dehydration of MCPM

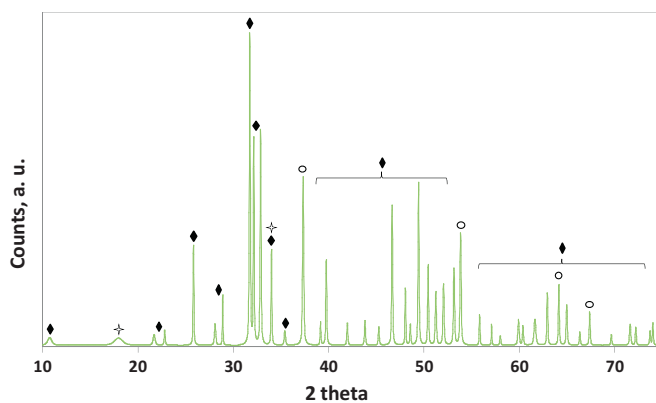


Fig. 4. XRD patterns of Ca-HA powder after 48 h of reaction, which was calcined at 1000°C for 2 h. Principal diffractions of Ca-HA (◆); CaO (○); $\text{Ca}(\text{OH})_2$ (+).

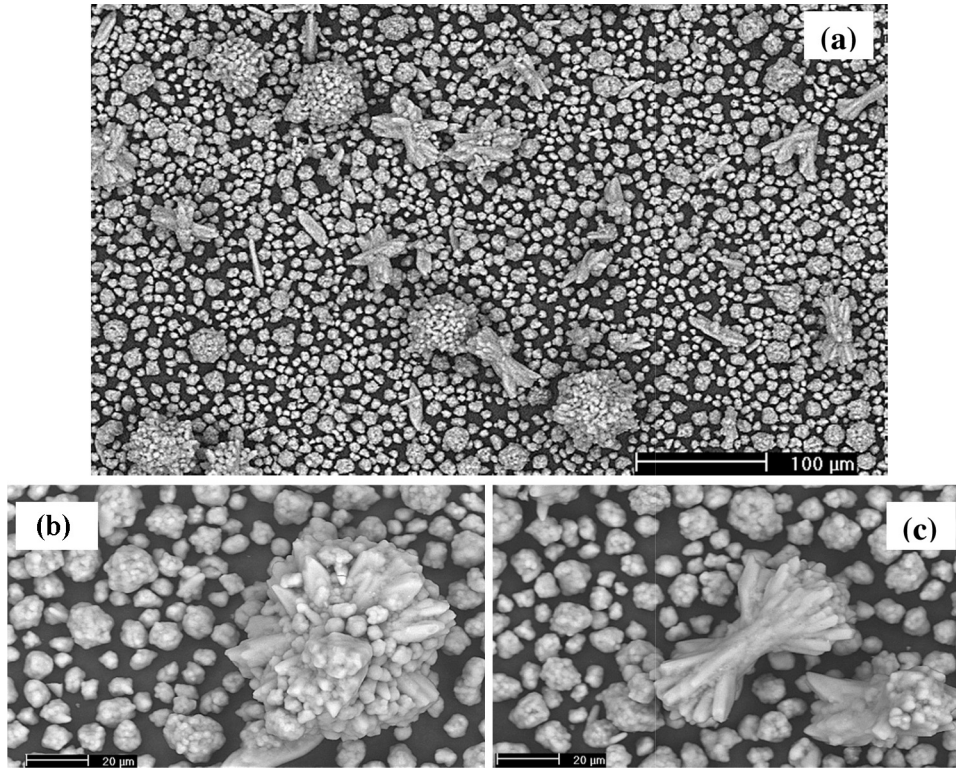


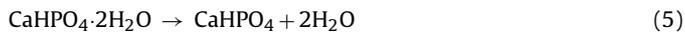
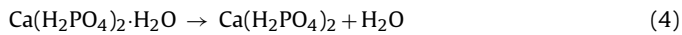
Fig. 5. SEM micrographs of Ca-HA powder after 48 h of reaction and drying at 105 °C, (a) general morphology, (b) and (c) detailed morphology.

Table 4

Elemental analysis of Ca-HA powder obtained after 48 h of reaction by EDX analysis (depth of EDX analysis of 1 µm).

	Atomic %					Molar ratio of Ca to P	
	C	O	P	K	Ca		
Large particles (>30 µm)	29.5 ± 3.7	44.0 ± 7.0	9.6 ± 1.3	0.7 ± 0.3	16.3 ± 2.7	1.7 ± 0.1	Average Ca/P 2.1 ± 0.7
Small particles (<30 µm)	38.4 ± 6.7	43.9 ± 3.8	4.5 ± 0.5	0.2 ± 0	13.0 ± 3	2.9 ± 0.5	

(Ca(H₂PO₄)₂·H₂O), which was still present after 2 h of reaction (Eq. (4)). DCPD (or brushite, CaHPO₄·2H₂O) was the most important intermediate after 2 h of reaction (Eq. (5)), as shown by its dehydration between 155 and 230 °C (≈ 4%) to form monetite (DCPA, CaHPO₄):

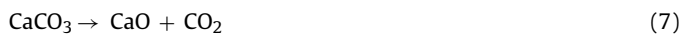


The monetite is then thermally transformed into calcium pyrophosphate (Ca₂P₂O₇) between 365 and 510 °C (≈ 2%) following Eq. (6).



For the samples after 24 h and 48 h of reaction, these intermediates were not significantly detected by TG analysis, indicating that the synthesis reached equilibrium after 24–48 h of reaction.

For all the samples, the main weight loss observed between 550 and 830 °C corresponds to the release of carbon dioxide gas (Eq. (7)) as the result of the decarbonation of remaining calcium carbonate into quicklime (CaO).



Regarding the samples after 24 h and 48 h of reaction, a small weight loss between 800 and 900 °C can be observed. This could be attributed to the decarbonation of B-type carbonate apatite (CAP) [15,18].

From the TG results above, we could calculate the calcium carbonate content remaining in the solid products corresponding to its thermal decomposition between 550 and 830 °C (Table 3).

After 2 h of reaction, a half of CaCO₃ was converted into calcium phosphates. This is explained by a strong acid attack of calcium carbonate particles by phosphate solution at the beginning of the reaction. Then the decomposition of CaCO₃ is slowed down because of the increase of the pH to a neutral value (Fig. 1). A stable value of CaCO₃ content about 30% is obtained after 24–48 h of reaction under the chosen operating conditions. In addition, the precipitation of calcium phosphates during the reaction probably limits the contact between the particles of calcium carbonate and soluble phosphates, because of the formation of core-shell structure wherein remaining calcium carbonate was found in the core [10].

From the results in Tables 1 and 3, it can be observed that the conversions of both the reagents used (KH₂PO₄ and CaCO₃) were fairly close to each other. Other physico-chemical characterizations will focus on the solid product obtained after 48 h of reaction in order to evidence its different components.

3.4. XRD characterization

The diffractogram of Ca-HA powder obtained after 48 h of reaction and dried at 105 °C is presented in Fig. 3. Remaining calcite could be clearly observed with its fine and intense peak at 29.4°. This calcite is the crystal form of calcium carbonate (CaCO₃) used for Ca-HA synthesis. Different calcium phosphates were also observed.

Low crystallinity Ca-HA appeared as the main calcium phosphate with its principal diffraction peak at 32° . This last one is a spread out peak, which is typical of a poorly crystalline phase. The low crystallinity of calcium phosphates based components is due to the moderate reaction temperature of synthesis, ca. 25°C . Higher temperatures are required for the formation of well-crystallized Ca-HA [19,20]. To highlight the presence of Ca-HA as the main calcium phosphate, the synthesized solid was calcined at 1000°C for 2 h. The XRD pattern of this calcined solid is presented in Fig. 4. Stoichiometric hydroxyapatite was clearly observed. Lime (CaO) and portlandite ($\text{Ca}(\text{OH})_2$) were present as the results of the decarbonation of the remaining calcite at 1000°C .

In addition to Ca-HA, B-type calcium-carbonate apatite (B-type CAP, formed by the substitution of PO_4^{3-} groups by CO_3^{2-} groups) seemed to be detected but at much lower amounts. The formation of carbon dioxide from the dissolution of calcite, associated with the increase of pH favored this substitution. This feature has been highlighted by IR analysis in a previous study [10]. The presence of CAP is in agreement with the TG analysis presented above. Octacalcium phosphate (OCP, $\text{Ca}_8\text{H}_2(\text{PO}_4)_6 \cdot 5\text{H}_2\text{O}$), was also formed in small amounts, evidenced by its main peak at 4.7° . OCP is known as an intermediate state during the formation of Ca-HA in an aqueous solution [18].

3.5. SEM-EDX analysis

The Ca-HA powder obtained after 48 h of reaction was examined by SEM and some examples are presented in Fig. 5. In parallel, EDX analysis was also performed. For spot mode of analysis, a volume of about $1\ \mu\text{m}^3$ was analyzed ($1\ \mu\text{m} \times 1\ \mu\text{m} \times 1\ \mu\text{m}$). In all cases, EDX analysis showed the presence of Ca, P, O, K and C (Table 4). Potassium was only found in trace amounts. Carbon came from the remaining calcium carbonate, carbonic gas in air and CAP formed during reaction. Ca, P, and O were the main elements of calcium phosphates and/or calcium carbonate.

Different morphologies were observed (Fig. 5a). The first population includes large spherical-like agglomerates consisting of needle-like assembled particles ($>30\ \mu\text{m}$), which seemed to be the result of the agglomeration of smaller particles, as highlighted in Fig. 5b and c. These morphologies would be characteristic of hydroxyapatite phase [21,22]. EDX analysis of these large particles, repeated on more than 15 particles, showed the atomic ratio of Ca to P equal to 1.7. This ratio is close to that of stoichiometric hydroxyapatite (Table 4). The calculated standard deviation was low (Table 4), which suggests that the surface of large particles have a good homogeneity (for the depth of EDX analysis of $1\ \mu\text{m}$).

The second population consists in spherical-like particles smaller than $30\ \mu\text{m}$. EDX analysis was also performed on these particles (Table 4). The result showed an average atomic ratio of Ca to P of 2.9, with a high standard deviation. So the surface of these particles was more heterogeneous in terms of chemical composition, compared to large particles. EDX beam might reach the core of small particles, where are located the remaining calcium carbonates [15]. Consequently, the atomic ratio of Ca to P is higher due to the presence of CaCO_3 . The average atomic ratio of Ca to P of both populations was equal to 2.1.

3.6. XPS analysis

The XPS analysis was conducted on an elliptical surface of $400\ \mu\text{m} \times 200\ \mu\text{m}$ with the depth of 10 nm. Taking into account the size of the particles scanning by electron microscopy (average mean diameter of particles, d_{50} of $24.2\ \mu\text{m}$, Table 6 in the next section), the atomic percentages calculated by semi-quantitative XPS analysis corresponds to the average obtained on a powder bed. Therefore, it is not possible to discriminate the composition of different

Table 5

Comparison of atomic ratio of Ca to P obtained by different methods for the solid powder after 24 h of reaction.

Method	Depth of analysis	Molar ratio of Ca to P
ICP-AES	Bulk analysis	2.4
SEM-EDX	Around 1000 nm	2.1
XPS	Around 10 nm	1.5

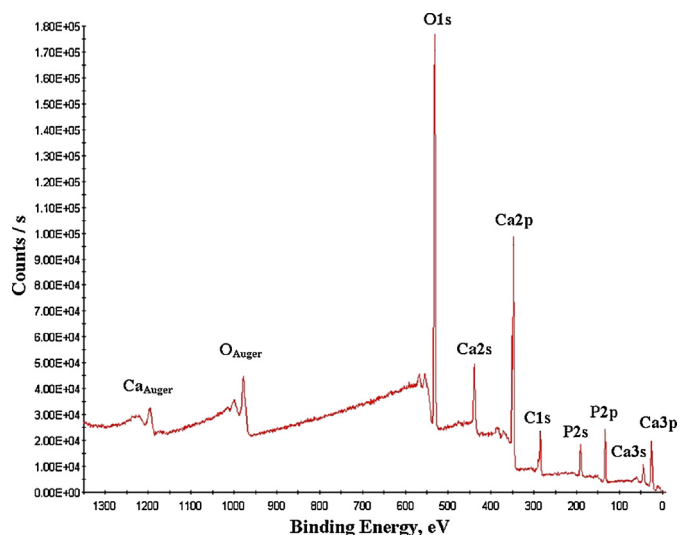


Fig. 6. XPS spectrum of Ca-HA powder obtained after 48 h of reaction.

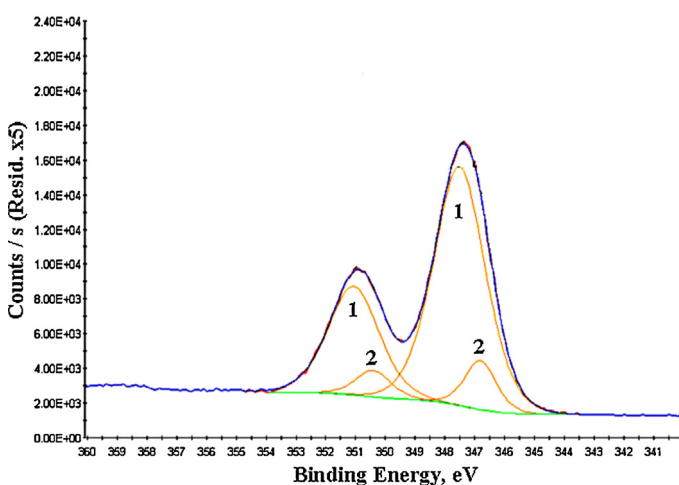


Fig. 7. Peak deconvolution for the signal of Ca2p; 1: apatitic calcium phosphate; 2: calcium carbonate.

morphologies of particles as done with SEM-EDX. Fig. 6 shows the XPS spectrum of Ca-HA powder obtained after 48 h of reaction.

Oxygen (O1s), calcium (Ca2p), phosphorus (P2p) and carbon (C1s) were detected as the major elements. The atomic content of these elements, determined by XPS analysis, were 13.1, 20.3, 50.5 and 16.1% for P2p, Ca2p, O1s and C1s, respectively. The peak of the carbon C1s at $284.6\ \text{eV}$ could be attributed to the remaining calcium carbonate, to CAP, and to surface contamination. For Ca2p, peak deconvolution between 344 and $354\ \text{eV}$ shows the major contribution of apatitic calcium phosphate (maximum of peak at 347.5 and $351\ \text{eV}$) for the first layers of surface (Fig. 7). Peaks corresponding to calcium carbonate (maximum of peak at 346.8 and $350.4\ \text{eV}$) had smaller intensity. On the other hand, the distinction of

Table 6
Physical properties of the solid powder obtained after 48 h of reaction.

S_{BET} , $\text{m}^2 \text{g}^{-1}$	d_{50} , μm	True density, g cm^{-3}	d_{pores} , nm	Porosity, %
148	24.2	2.74	11	61

different phosphocalcic phases present in the sample, i.e. Ca-HA, OCP, DCPD, CAP, remains difficult [23].

Table 5 compares the atomic ratio of Ca to P determined by different methods. A decrease of the atomic ratio of Ca to P from the core to the surface of the solid particles was observed. In fact, the remaining calcium carbonate must be found in the core of particles, as previously evidenced by Pham Minh et al. [10]. In addition, apatitic calcium phosphate contains usually hydrogenophosphate groups (HPO_4^{2-}) on its surface, when it was in contact with the humidity in air. This surface would be similar to a mixture of phosphocalcic species including DCPD, DCPA and OCP, which have the molar ratio of Ca to P smaller than 1.67 [24].

3.7. Physical characterizations

Physical characterizations of the solid powder obtained after 48 h of reaction are presented in Table 6. Despite the incomplete conversion of the initial calcium carbonate, this solid powder had a high specific surface area (S_{BET}) of $148 \text{ m}^2 \text{g}^{-1}$. This specific surface area could be explained by the presence of mesopores with the average mean diameter of pores of 11 nm, obtained by nitrogen adsorption. The average mean diameter of particles obtained by laser scattering was $24.2 \mu\text{m}$, confirming the results of SEM analysis. Finally, this solid had the true density of 2.74 g cm^{-3} , usually found for a given calcium phosphate synthesized at moderate temperature.

3.8. Reactivity of the solid powder during Zn^{2+} removal

This section communicates the results on the removal of Zn^{2+} from an aqueous solution using the solid powder obtained after 48 h of reaction. As mentioned above, the solid sorbent was filtered, washed, dried at 105°C and then ground before sorption experiment. The initial solid sorbent is thereafter called Ca-HA-P before sorption experiment. The solid recovered after sorption experiment is called Ca-HA-P-Zn.

3.8.1. Kinetic study

Fig. 8 shows the evolution of the concentration of the different elements present in solution as well as pH, for an initial

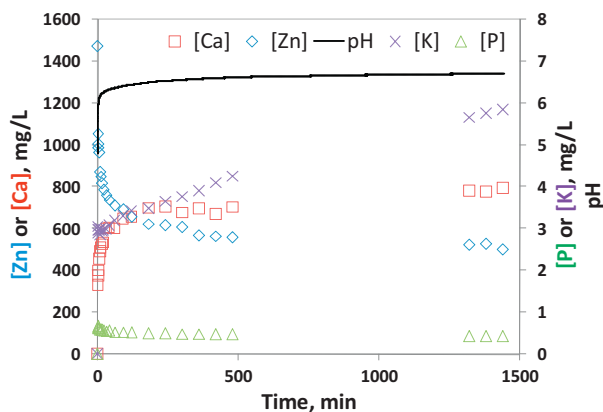


Fig. 8. Evolution of pH and concentration of the soluble Zn, Ca, P, K in solution as a function of contact time during batch sorption experiment. Sorption conditions: 1 L of 1500 ppm of Zn^{2+} , 8 g of Ca-HA-P, room temperature.

concentration of Zn of 1500 mg L^{-1} . The initial pH of zinc nitrate solution was close to 4.9. It rapidly increased to 6 after only 2 min of contact with calcium phosphate powder. This increase was probably induced by the buffering capacity of apatitic calcium phosphates [25], and also of calcium carbonate remaining in the solid sorbent. Then, the pH evolved slowly to the final value of 6.7 after 24 h of reaction.

For the evolution of the concentration of the soluble elements in the sorption medium, we observe that the kinetic of calcium release to the liquid was equivalent to that of Zn removal from the liquid. A rapid decrease of Zn concentration in the first minutes of sorption was observed. 30 and 43% of Zn were removed after respectively 1 and 10 min of reaction. Then the sorption yield slowed down strongly after 5 h of reaction time. This kinetic profile is typical for the sorption of a given metal using Ca-HA based sorbent in batch reactor [7,26]. After 24 h of reaction, the concentration of Zn remaining in the solution was around 500 ppm, corresponding to the removal yield of 66% of the Zn present and the sorption capacity of 118 mg of Zn per g of sorbent. In parallel with Zn removal, calcium was quickly released to the liquid phase during the first minutes of reaction. Its concentration was 700 ppm after 180 min of contact time and finally reached 800 ppm after 24 h of reaction.

Soluble phosphorus and potassium were found at much lower concentrations. Soluble phosphorus did not exceed 1 ppm along the sorption experiment. The low concentration of soluble phosphate species is explained by the abundance of divalent cations (Ca^{2+} and Zn^{2+}) in the reaction medium. The concentration of soluble potassium varied between 3 and 6 ppm.

In order to evaluate the sorption rate of Zn^{2+} , a pseudo-second order kinetic model was applied to the results in Fig. 8 [27]. This model is described as follows:

$$\frac{t}{Q_t} = \frac{1}{h} + t \times \frac{1}{Q_e} \quad (8)$$

where Q_t and Q_e is the amount of Zn sorbed on Ca-HA at any time t and at equilibrium respectively (mg g^{-1}), t is the contact time (min) and h is the constant of sorption rate ($\text{g mg}^{-1} \text{min}^{-1}$).

The plot of t/Q_t against the contact time t allows determining the values of Q_e and h (Table 7). The value of R^2 close to 1 indicates that the experimental data of Zn sorption matches well with the pseudo-second order kinetic model. The value of Q_e obtained from the model (123 mg g^{-1}) is close to that from the sorption experiment (118 mg g^{-1}).

Table 8 compares the performance of the Ca-HA based sorbent in this work with other Ca-HA reported in the literature for the removal of Zn^{2+} . Starting from CaCO_3 and KH_2PO_4 , Ca-HA sorbent

Table 7

Sorption capacity (Q_e), rate constant (h) and correlation coefficients (R^2) of synthesized Ca-HA calculated from the pseudo-second order sorption kinetic model.

	Q_e , mg g^{-1}	h , $\text{g mg}^{-1} \text{min}^{-1}$	R^2
Ca-HA-P	123	6.2×10^{-4}	0.9993

Table 8

Comparative sorption capacity (Q_e) of the synthesized Ca-HA sorbent in this work with other Ca-HA sorbents reported in the literature in the sorption of zinc(II) from aqueous solution.

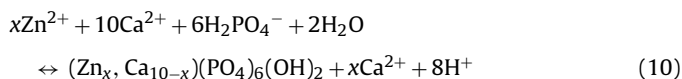
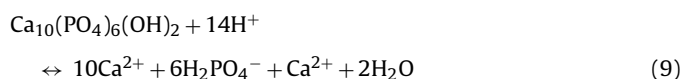
Ca-HA, g L^{-1}	Zinc, mg L^{-1}	Q_e , mg g^{-1}	Ref.
8	1500	123	This work
10	1500	102	[5]
1	523	77	[26]
2	378	33	[16]
5	654	23	[28]
3.4	39	6	[30]
25	500	12	[29]

in this work had higher Q_e in comparison with Ca-HA made from soluble calcium salt like $\text{Ca}(\text{NO}_3)_2$ [5,16,26,28], as well as from phosphate rocks [29,30]. This may be explained by the low crystallinity of the Ca-HA synthesized in this work, which improves the physico-chemical properties of the sorbent (Table 6), i.e. high specific surface area, high porosity and small particle size. The low crystallinity of Ca-HA was due to the soft synthesis conditions of the sorbent (at 25 °C under atmospheric pressure), as well as the use of calcium carbonate as the non-conventional calcium source. This last one promotes the presence of gaps and impurities (CO_3^{2-} ion insertion in Ca-HA structure), improving the sorption properties of Ca-HA [31].

3.8.2. Discussion on sorption mechanism

According to the literature, several sorption mechanisms were proposed to occur simultaneously and/or successively. Ionic exchange, surface complexation reaction and dissolution-precipitation are the three main mechanisms invoked in the sorption process of Zn by Ca-HA based materials [16,32,33].

The dissolution-precipitation mechanism consists in two successive steps, the first one is the dissolution of Ca-HA in an acid medium (Eq. (9)), followed by the precipitation of Zn phosphate (Eq. (10)). H_2PO_4^- is expected as the main soluble phosphate species in the solution, taking into account the pH profile of the reaction medium (4.9–6.7) [10]. However, the low concentration of the soluble phosphate species (Fig. 8) suggests that this mechanism is only marginal, as usually observed in the literature [26]. In addition, XRD analysis did not show the formation of apatitic calcium-zinc-phosphate solid solution (data not shown).



In the case of Zn removal at high initial concentration, the formation of hopeite (hydrated Zn phosphate, $\text{Zn}_3(\text{PO}_4)_2 \cdot 4\text{H}_2\text{O}$) might also take place, as illustrated in Eq. (11) [33–35]. TG analysis of the solid recovered after sorption experiment (Ca-HA-P-Zn) evidenced the presence of hopeite (Fig. 9). The weight loss between 125 and 200 °C (around 1 wt.%) was attributed to the first dehydration of hopeite, followed by its second dehydration between 200 and 340 °C (around 2 wt.%) to form anhydrous hopeite [36]. Taking into account the pH profile of the sorption medium, we suppose that the dissolution-precipitation mechanism might have occurred at the beginning of the sorption experiment, when the pH was lowest, which is favorable for the dissolution step. Fig. 9 evidenced

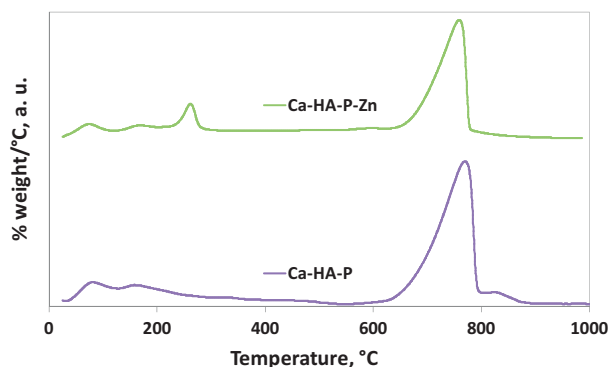


Fig. 9. Derivatives thermogravimetric (DTG) curves of Ca-HA-P and Ca-HA-P-Zn.

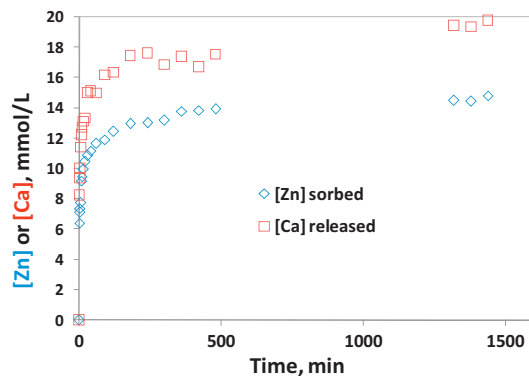
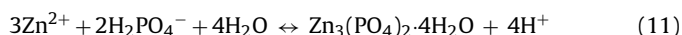
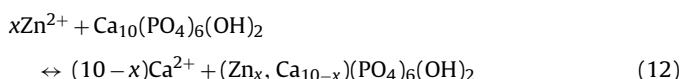


Fig. 10. Evolution of removed Zn^{2+} and released Ca^{2+} in batch sorption experiment. Sorption conditions: 1 L of 1500 ppm of Zn^{2+} , 8 g of Ca-HA-P, room temperature.

also the participation of CAP to the removal of Zn^{2+} . The decarbonation of B-type CAP at 800–900 °C disappeared from the TG curve of Ca-HA-P-Zn. In fact, the insertion of carbonate groups into the apatite structure increases the solubility of Ca-HA and promotes the presence of gaps in the apatitic structure [18]. Thus, a preferential dissolution of these carbonates groups may be assumed, releasing phosphate groups to the benefit of zinc phosphate precipitation. B-type CAP has been found to be more active for metal removal compared to Ca-HA [31].



The ion-exchange mechanism can be described by Eq. (12) [32]. The equimolar ion exchange is expected, and there is no release of protons in solution. However, this mechanism could not occur alone, because of the difference in the concentration of the released calcium and that of the removed Zn (Fig. 10). In Fig. 10, we observe that the molar concentration of the released calcium was always higher than that of the removed Zn. In addition, ion-exchange mechanism did not involve the release or consumption of protons, but the pH profile of the sorption medium changed along the sorption experiment (Fig. 8).



The surface complexation mechanism has been proposed by several authors in the literature [8,37]. According to Wu et al. [38], for a pH between 4.8 and 6, the main surface groups of an apatitic calcium phosphate are $\equiv\text{POH}$ and $\equiv\text{CaOH}_2^+$. So the surface complexation mechanism can be described by Eqs. (13) and (14). As shown in Fig. 11, a drop in pH profile during the first seconds

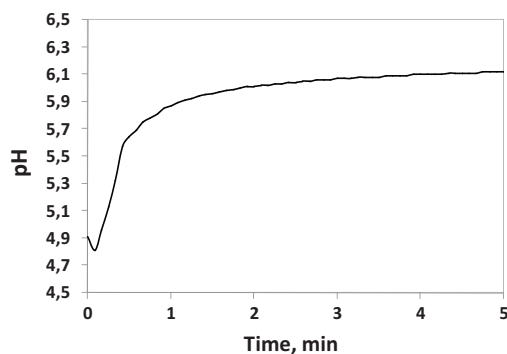


Fig. 11. pH evolution during the first 5 min of sorption experiment. Sorption conditions: 1 L of 1500 ppm of Zn^{2+} , 8 g of Ca-HA-P, room temperature.

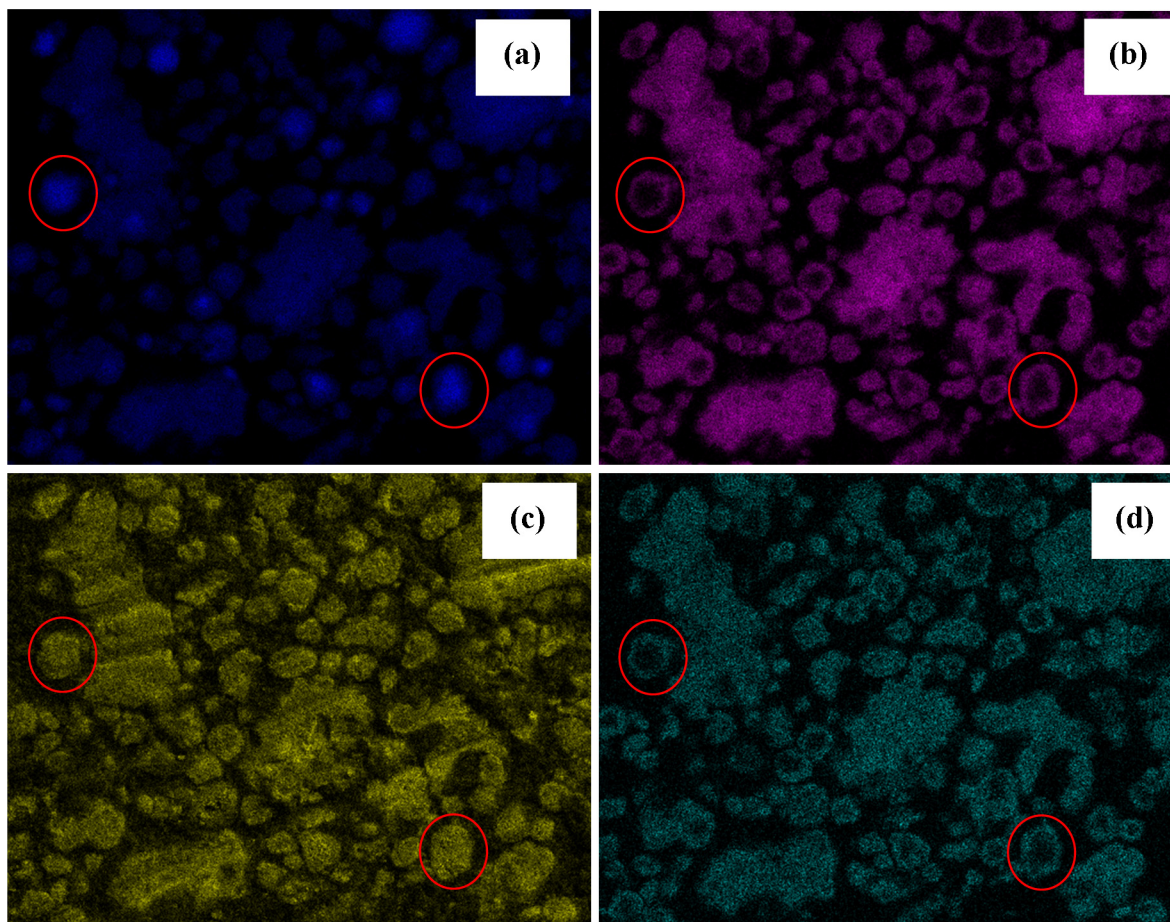
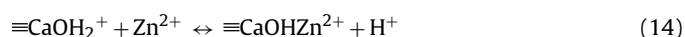


Fig. 12. Imaging of Ca-HA-P-Zn powder drying at 105 °C obtained by SEM-EDX analysis; (a) calcium, (b) phosphorus, (c) oxygen, (d) zinc. (Electronic version is required for a good observation of these images.)

of sorption experiment was observed. The surface complexation mechanism allowed explaining this drop of pH (Eqs. (13) and (14)).



In summary, all three mechanisms discussed above might take place during Zn^{2+} removal by Ca-HA starting with acid aqueous solutions. However, the pH profile and the concentration of soluble phosphate species allow confirming that dissolution-precipitation mechanism could happen marginally at the beginning of the sorption, wherein the pH was still sufficiently acid. The surface complexation must also start at the beginning of the reaction, leading to the decrease of pH during the first seconds of reaction. The surface complexation explains the non-equimolar exchange between Zn^{2+} and Ca^{2+} , observed in Fig. 10, according to Eqs. (13) and (14). Of course, the eventual acid attack on the remaining calcite particles, leading to the release of Ca^{2+} to the solution, explains also the higher concentration of the released Ca^{2+} compared to the concentration of the removed Zn^{2+} . The ion-exchange mechanism might also occur, in parallel with other processes because of the driving force of the sorption medium. The driving force is the difference in solubility between Ca-HA and Zn-doped Ca-HA newly formed (Ca-HA-P-Zn) [18,39,40]. In our case, the solubility product K_s of the initial Ca-HA and of the final solid recovered from the sorption experiment (Ca-HA-P-Zn) was measured. Ca-HA-P-Zn had lower solubility (K_s : 5.43×10^{-99}) than that of the initial Ca-HA (K_s : 1.78×10^{-94}). This favors the ion-exchange between Zn^{2+} from the solution with Ca^{2+} from apatitic matrix. This ion-exchange is

expected for a slow sorption kinetic. However, we cannot conclude that a solid solution was formed, as no differences in cell parameters were detected. An amorphous surface deposit of zinc phosphate could explain the result of ion exchange. About the formation of hopeite, the acid pH might cause the local dissolution of the phosphocalcic hydroxyapatite (Ca^{2+} , PO_4^{3-} , OH^-). This promotes the formation of heterogeneous precipitate, i.e. hopeite, under acid pH and with high initial concentration of Zn.

Regarding now the localization of Zn, fixed by the Ca-HA sorbent. Fig. 12 shows the imaging of the main elements present in the used sorbent. As expected, calcium was well located in the core of particles (Fig. 12A), probably in form of CaCO_3 . In fact, phosphorus was usually not present in the core of particles (Fig. 12B). Oxygen was present in the entire particles because oxygen is the component of both the remaining calcium carbonate and the calcium/zinc phosphates. Finally, Zn was only found on the surface of particles. This last confirms that the fixation of Zn by Ca-HA based particles was governed by surface processes, as discussed above.

4. Conclusions

Ca-HA based sorbent has been synthesized from calcium carbonate (calcite, CaCO_3) and potassium dihydrogen orthophosphate (KH_2PO_4) at moderate conditions. Apatitic Ca-HA based sorbent of low crystallinity was formed. The intermediates of the synthesis reaction have been identified as mainly MCPM, DCPD and OCP. The characterization of the final product showed the presence of apatitic compounds including Ca-HA, B-type CAP, OCP, and unreacted calcium carbonate as the main components. Remaining

calcium carbonate was found in the core of particles. The elemental analysis of the sorbent by three different methods (ICP-AES, SEM-EDX, and XPS) evidenced the decrease of the molar ratio of Ca to P from the core to the surface of particles. The average size of the final solid sorbent was 24.2 μm . Two populations of particles were observed. The first one was composed of particles smaller than 30 μm . The second one included big agglomerates of tens of μm . Under soft synthesis conditions, the final solid sorbent had high specific surface area (148 $\text{m}^2 \text{g}^{-1}$), associated with mesopores (average mean diameter of 11 nm).

This solid sorbent had high reactivity for the removal of Zn^{2+} from an aqueous solution, with the sorption capacity (Q_e) of 118 mg of Zn^{2+} per g of sorbent. This high performance is explained by the high specific surface area and porosity, the low crystallinity of the sorbent, and the presence of gaps and impurities (CO_3^{2-} ions) in the apatitic structure of the sorbent. The mechanisms of Zn uptake were also discussed, which were surface processes.

This study demonstrated a simple route for the production of Ca-HA based sorbent from economical starting materials. The high performance of this synthesized sorbent in the sorption of Zn opens new prospects on the valorization of carbonate and phosphate industrial wastes for environmental purposes and for wastewater remediation in particular.

Acknowledgments

The authors gratefully acknowledge the scientific and financial support of Solvay Group (Belgium) and colleagues at RAPSODEE Centre, Christine Rolland, Céline Boachon, Jean-Marie Sabathier, for their technical help.

References

- [1] X. Chen, J.V. Wright, J.L. Conca, L.M. Peurrung, Evaluation of heavy metal remediation using mineral apatite, *Water Air Soil Pollut.* 98 (1997) 57–78.
- [2] A. Nzihou, P. Sharrock, Role of phosphate in the remediation and reuse of heavy metal polluted wastes and sites, *Waste Biomass Valoriz.* 1 (2010) 163–174.
- [3] A. Nzihou, P. Sharrock, Calcium phosphate stabilization of fly ash with chloride extraction, *Waste Manage.* 22 (2002) 235–239.
- [4] D.W. Bostick, Use of Apatite for Chemical Stabilization of Subsurface Contaminants, 2003 <http://www.osti.gov/servlets/purl/820754-Fk9X7K/native/> (accessed 10.06.15).
- [5] R.R. Sheha, Sorption behavior of $\text{Zn}(\text{II})$ ions on synthesized hydroxyapatites, *J. Colloid Interface Sci.* 310 (2007) 18–26.
- [6] Q.Y. Ma, S.J. Traina, T.J. Logan, J.A. Ryan, Effects of aqueous Al, Cd, Cu, Fe(II), Ni, and Zn on Pb immobilization by hydroxyapatite, *Environ. Sci. Technol.* 28 (1994) 1219–1228.
- [7] M. Fedoroff, J. Jeanjean, J.C. Rouchaud, L. Mazerolles, P. Trocellier, P. Maireles-Torres, et al., Sorption kinetics and diffusion of cadmium in calcium hydroxyapatites, *Solid State Sci.* 1 (1999) 71–83.
- [8] S. Baille, A. Nzihou, D. Bernache-Assolant, E. Champion, P. Sharrock, Removal of aqueous lead ions by hydroxyapatites: equilibria and kinetic processes, *J. Hazard. Mater.* 139 (2007) 443–446.
- [9] H. Sebei, N. Lyczko, D. Pham Minh, A. Nzihou, P. Sharrock, Valorization of carbonate waste as hydroxyapatite for heavy metals remediation, in: 4th International Conference on Engineering for Waste and Biomass Valorisation (Porto Portugal), vol. 2, 2012, pp. 578–585, ISBN: 979-10-91526-00-5.
- [10] D. Pham Minh, N. Lyczko, H. Sebei, A. Nzihou, P. Sharrock, Synthesis of calcium hydroxyapatite from calcium carbonate and different orthophosphate sources: a comparative study, *Mater. Sci. Eng. B* 177 (2012) 1080–1089.
- [11] D. Pham Minh, N.D. Tran, A. Nzihou, P. Sharrock, One-step synthesis of calcium hydroxyapatite from calcium carbonate and orthophosphoric acid under moderate conditions, *Ind. Eng. Chem. Res.* 52 (2013) 1439–1447.
- [12] Y. Hashimoto, T. Sato, Removal of aqueous lead by poorly-crystalline hydroxyapatites, *Chemosphere* 69 (2007) 1775–1782.
- [13] M. Pomiès, J.M. Choubert, M. Coquery, Devenir des métaux au sein des stations d'épuration – Analyse d'une base de données spécifique, 2009 http://www.onema.fr/IMG/pdf/2009_030.pdf (accessed 10.06.15).
- [14] R.A. Barrea, C.A. Pérez, A.Y. Ramos, H.J. Sánchez, M. Grénón, Distribution and incorporation of zinc in biological calcium phosphates, *X-ray Spectrom.* 32 (2003) 387–395.
- [15] D. Pham Minh, H. Sebei, A. Nzihou, P. Sharrock, Apatitic calcium phosphates: synthesis, characterization and reactivity in the removal of lead(II) from aqueous solution, *Chem. Eng. J.* 198–199 (2012) 180–190.
- [16] M. Peld, K. Tönsuaadu, V. Bender, Sorption and desorption of Cd^{2+} and Zn^{2+} ions in apatite-aqueous systems, *Environ. Sci. Technol.* 38 (2004) 5626–5631.
- [17] W.F. Neuman, T.Y. Toribara, B.J. Mulryan, Synthetic hydroxyapatite crystals I. Sodium potassium fixation, *Arch. Biochem. Biophys.* 98 (1962) 384–390.
- [18] J.C. Elliott, Structure and Chemistry of the Apatites and Other Calcium Orthophosphates, Elsevier, 1994.
- [19] M. Yoshimura, P. Sujaridworakun, F. Koh, T. Fujiwara, D. Pongkao, A. Ahniyaz, Hydrothermal conversion of calcite crystals to hydroxyapatite, *Mater. Sci. Eng. C* 24 (2004) 521–525.
- [20] S. Jinawath, D. Pongkao, W. Suchanek, M. Yoshimura, Hydrothermal synthesis of monetite and hydroxyapatite from monocalcium phosphate monohydrate, *Int. J. Inorg. Mater.* 3 (2001) 997–1001.
- [21] R.Z. LeGeros, Calcium phosphates in oral biology and medicine, *Monogr. Oral Sci.* 15 (1991) 1–201.
- [22] R.N. Panda, M.F. Hsieh, R.J. Chung, T.S. Chin, FTIR, XRD, SEM and solid state NMR investigations of carbonate-containing hydroxyapatite nano-particles synthesized by hydroxide-gel technique, *J. Phys. Chem. Solids* 64 (2003) 193–199.
- [23] B. Demri, D. Muster, XPS study of some calcium compounds, *J. Mater. Process. Technol.* 55 (1995) 311–314.
- [24] Å. Bengtsson, Solubility and Surface Complexation Studies of Apatites, Umeå University, Sweden, 2007 (Ph.D. dissertation).
- [25] I.D. Smičiklas, S.K. Milonjić, P. Pfendt, S. Raičević, The point of zero charge and sorption of cadmium (II) and strontium (II) ions on synthetic hydroxyapatite, *Sep. Purif. Technol.* 18 (2000) 185–194.
- [26] A. Corami, S. Mignardi, V. Ferrini, Copper and zinc decontamination from single- and binary-metal solutions using hydroxyapatite, *J. Hazard. Mater.* 146 (2007) 164–170.
- [27] Y.S. Ho, G. McKay, A comparison of chemisorption kinetic models applied to pollutant removal on various sorbents, *Process Saf. Environ. Prot.* 76 (1998) 332–340.
- [28] I. Smičiklas, A. Onjia, S. Raičević, Đ. Janačković, M. Mitrić, Factors influencing the removal of divalent cations by hydroxyapatite, *J. Hazard. Mater.* 152 (2008) 876–884.
- [29] Z. Elouear, J. Bouzid, N. Boujelben, M. Feki, F. Jamoussi, A. Montiel, Heavy metal removal from aqueous solutions by activated phosphate rock, *J. Hazard. Mater.* 156 (2008) 412–420.
- [30] X. Cao, L.Q. Ma, D.R. Rhue, C.S. Appel, Mechanisms of lead, copper, and zinc retention by phosphate rock, *Environ. Pollut.* 131 (2004) 435–444.
- [31] M. Miyake, K. Watanabe, Y. Nagayama, H. Nagasawa, T. Suzuki, Synthetic carbonate apatites as inorganic cation exchangers. Exchange characteristics for toxic ions, *J. Chem. Soc. Faraday Trans.* 86 (1990) 2303–2306.
- [32] Y. Xu, F.W. Schwartz, S.J. Traina, Sorption of Zn^{2+} and Cd^{2+} on hydroxyapatite surfaces, *Environ. Sci. Technol.* 28 (1994) 1472–1480.
- [33] Y.J. Lee, E.J. Elzinga, R.J. Reeder, Sorption mechanisms of zinc on hydroxyapatite: systematic uptake studies and EXAFS spectroscopy analysis, *Environ. Sci. Technol.* 39 (2005) 4042–4048.
- [34] C. Stötzel, F.A. Müller, F. Reinert, F. Niederdraenk, J.E. Barralet, U. Gbureck, Ion adsorption behaviour of hydroxyapatite with different crystallinities, *Colloids Surf. B: Biointerfaces* 74 (2009) 91–95.
- [35] Chen, J.V. Wright, J.L. Conca, L.M. Peurrung, Effects of pH on heavy metal sorption on mineral apatite, *Environ. Sci. Technol.* 31 (1997) 624–631.
- [36] L. Herschke, Polymer Controlled Mineralization of Zinc Phosphate Hydrates and Applications in Corrosion Protection, Catalysis and Biomedicine, Johannes Gutenberg University of Mainz, Germany, 2004 (Ph.D. dissertation).
- [37] E. Mavropoulos, A.M. Rossi, A.M. Costa, C.A.C. Perez, J.C. Moreira, M. Saldanha, Studies on the mechanisms of lead immobilization by hydroxyapatite, *Environ. Sci. Technol.* 36 (2002) 1625–1629.
- [38] L. Wu, W. Forsling, P.W. Schindler, Surface complexation of calcium minerals in aqueous solution: 1. Surface protonation at fluorapatite–water interfaces, *J. Colloid Interface Sci.* 147 (1991) 178–185.
- [39] J.O. Nriagu, Lead orthophosphates—II. Stability of chlopyromophite at 25 °C, *Geochim. Cosmochim. Acta* 37 (1973) 367–377.
- [40] Y. Takeuchi, T. Suzuki, H. Arai, A study of equilibrium and mass transfer in processes for removal of heavy-metal ions by hydroxyapatite, *J. Chem. Eng. Jpn.* 21 (1988) 98–100.